*Journal of Thermal Analysis and Calorimetry, Vol. 77 (2004) 639–652*

# SOLID-STATE FORMS OF PRILOCAINE HYDROCHLORIDE
## Crystal polymorphism of local anaesthetic drugs, Part II

*A. C. Schmidt, V. Niederwanger and U. J. Griesser*[*]

Institute of Pharmacy, Ph. Technology, University of Innsbruck, Innrain 52, 6020 Innsbruck, Austria

## Abstract

Two polymorphic forms, a dioxane solvate and the amorphous form of the local anaesthetic drug prilocaine hydrochloride (N-(2-methylphenyl)-2-propylamino monohydrochloride, PRCHC) were characterized by thermal analysis (hot stage microscopy, differential scanning calorimetry, thermogravimetry), vibrational spectroscopy (FTIR, FT-Raman-spectroscopy), powder X-ray diffractometry and water vapor sorption analysis. The formation and thermodynamic stability of the different solid phases is described and presented in a flow chart and an energy temperature diagram, respectively. Mod. I° (*m.p*. 169°C) is the thermodynamically stable form at room temperature and present in commercial products. This form crystallizes from all tested solvents except 1,4-dioxane which gives a solvate with half a mole of 1,4-dioxane per mole PRCHC. Mod. II occurs only on desolvation of the dioxane solvate and shows a lower melting point (165.5°C) than mod. I° and a lower heat of fusion. Thus, according to the heat of fusion rule, mod. II is the thermodynamically less stable form in the entire temperature range (monotropism) but kinetically stable for at least a year. Freeze-drying of an aqueous solution leads to the amorphous form. On heating and in moist air amorphous PRCHC exclusively crystallizes to the stable mod. I°. PRCHC exemplifies that certain metastable polymorphic forms are only accessible via a specific solvate, but not via any other crystallization path. Since no crystallization from 1,4-dioxane was performed in earlier solid-state studies of this compound, PRCHC was to this date rated as monomorphic.

**Keywords:** crystal forms, crystal polymorphism, local anaesthetics, prilocaine hydrochloride, solid-state properties, solvate, thermal analysis

## Introduction

Local anaesthetic drugs (LA) represent a group of compounds with common structural features which determine their pharmacological profile. The hydrophilic end group (tertiary or secondary amine) is responsible for the receptor binding of the molecule whereas the lipophilic group (aromatic ring system) affects the duration of action [1]. These essential groups are mostly linked by an ester or amide bridge. One result of our systematic investigations on the solid-state properties of numerous local anaesthetic

* Author for correspondence: E-mail: ulrich.griesser@uibk.ac.at

*1388–6150/2004/ $ 20.00*

*Akadémiai Kiadó, Budapest*
*Kluwer Academic Publishers, Dordrecht*

drugs is that particularly LA of the ester type show many cases of polymorphism [2–6], whereas the amide type LA tend to form also hydrates or solvates [7, 8].

The present paper deals with the solid-state characterization of prilocaine hydrochloride (PRCHC), a local anaesthetic drug of the amide type (Fig. 1). The compound is official in the United States Pharmacopoeia (USP) and the Pharmacopoeia Europaea and is therapeutically used for intravenous regional anaesthesia and in dentistry where it shows a medium duration of action compared to other local anaesthetic drug compounds [9].

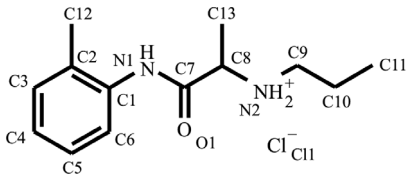


**Fig. 1** Molecular structure of PRCHC with atom numbers

In none of the previous analytical studies dealing with the solid-state properties of PRCHC [10, 11] the existence of different solid-state forms has been mentioned. Moreover, in the Cambridge Structural Database the crystal structures of all frequently used LA of the amide type can be found, such as Lidocaine [12], Lidocaine hydrochloride monohydrate [13], Dibucaine hydrochloride monohydrate [14], Mepivacaine hydrochloride, Bupivacaine hydrochloride [15], Bupivacaine hydrochloride ethanol solvate [16], Ropivacaine hydrochloride monohydrate [15], Phenacaine hydrochloride monohydrate (an amidine) [17] but not that of PRCHC. The hydrochloride salts of these compounds mostly crystallize in the space group $P2_1$ and the organization or molecular packing in the crystals show pronounced similarities. Moreover, the protonated drug molecules in all cases (amide type and ester type LA) are linked by hydrogen bonds via the chloride anions forming parallel orientated, infinitive hydrogen-bonded chains. The multiple occurrence of solvated forms within the group of the amide type LA is likely due to the ability to form intermolecular hydrogen bonds with the N1 amine group. The alkyl side chain of the PRCHC molecule may adopt different conformations. Such flexible aliphatic side chains are relevant for the formation of different (conformational) polymorphs and this is a common structural feature of local anaesthetics.

In the present study, we describe the formation and the physical properties of new solid-state forms of PRCHC. Thermal analytical methods, vibrational spectroscopy, powder X-ray diffraction and water vapor sorption analysis were applied in order to identify and characterize the solid phases and to evaluate their relative thermodynamic and kinetic stabilities.

## Materials and methods

### *Materials*

PRCHC ‘Citanest chloride’ from Astra Op13 22-055-1 was available for this study. All solvents used in this study were of p.a. (‘pro analysis’) quality.

*Methods*

Hot-stage-microscopy

The thermal behavior of the solid-state forms were observed with a Reichert Thermovar® polarized microscope (Reichert, Vienna, A) equipped with a Kofler hot stage (Reichert, Vienna, A).

Differential scanning calorimetry (DSC)

DSC curves were recorded with a DSC 7 system (Perkin Elmer, Norwalk, Ct., USA) using the Pyris 2.0 software. Samples of approximately 2 mg (masses controlled to ±0.0005 mg using a UM3 ultramicrobalance, Mettler, Greifensee, CH) were weighed into Al pans (25 μL) with perforated cover. Dry nitrogen was used as purge gas (purge: 20 mL $min^{-1}$), calibrated with caffeine (236.4°C) and indium 99.999% (156.6°C, 28.45 J $g^{-1}$).

Infrared spectroscopy

Fourier transform infrared (FTIR) spectra were acquired on a Bruker IFS 25 spectrometer (Bruker Analytische Messtechnik GmbH, Karlsruhe, D). Spectra over a range of 4000 to 400 $cm^{-1}$ with a resolution of 2 $cm^{-1}$ (50 scans) were recorded on KBr tablets (approximately 2 mg PRCHC per 300 mg KBr). For temperature-controlled FTIR spectra the samples were prepared on ZnSe disks using a heating device (Bruker) and the Bruker IR microscope I (Bruker Analytische Messtechnik GmbH, Karlsruhe, D), with a 15× Cassegrain objective (spectral range 4000 to 600 $cm^{-1}$, resolution 4 $cm^{-1}$, 100 interferograms per spectrum).

Raman spectroscopy

Raman spectra of the forms were recorded with a Bruker RFS 100 Raman spectrometer (Bruker Analytische Messtechnik GmbH, Karlsruhe, D), equipped with a Nd:YAG Laser (1064 nm) as excitation source and a liquid-nitrogen-cooled, high-sensitivity Ge-detector. The spectra were recorded in aluminium sample holders at a laser power of 300 mW (64 scans per spectrum).

Powder X-ray diffractometry (PXRD)

The X-ray diffraction patterns were obtained using a Siemens D-5000 diffractometer (Bruker AXS, Karlsruhe, D) equipped with a theta/theta goniometer, a $CuK_\alpha$ radiation source, a Goebel mirror (Bruker AXS, Karlsruhe, D), a 0.15° soller slit collimator and a scintillation counter. The patterns were recorded at a tube voltage of 40 kV and a tube current of 35 mA, applying a scan rate of 0.005° 2θ $s^{-1}$ in the angular range of 2 to 40° in 2θ. Temperature- and moisture-controlled experiments were done with a low-temperature camera TTK (Anton Paar KG, Graz, A) and a SYCOS-H humidity control system (Asynco, Karlsruhe, D).

Water vapor sorption analysis

The moisture sorption isotherms were acquired using a SPS-11 moisture sorption analyzer (MD Messtechnik, Ulm, D). The measurement cycles were started at 0% relative humidity (RH) and increased in 10% steps up to 90% RH and back to 0% RH. The equilibrium condition for each step was set to a mass constance of ±0.007% over 40 min. The temperature was 25±0.1°C.

Lyophilization

Freeze-drying was performed with a Lyolab B, LSL (Secfroid Lyophilisator Inula, Wien, A) equipped with vacuum pump 2400 A (Alcatel Cit, Annecy Cedex, F). The frozen aqueous solutions (5%) were dried at a pressure of 0.05 mbar.

## Results and discussion

The crystal forms are named according to the Kofler notation using roman numerals in the order of the melting points (i.e. the form with the highest melting point is called mod. I). The modification which is thermodynamically stable at 20°C is marked with a superscript zero.

*Preparation of the different solid phases*

Mod. I°, the thermodynamically stable form at room temperature, is present in commercial products and crystallizes from a number of organic solvents, such as ethanol, methanol, ethylacetate, 2-propanol, acetone, *n*-butanol, toluol, $CHCl_3$, etc.

On recrystallization from 1,4-dioxane a solvate is obtained. This dioxane solvate contains half a mole of 1,4-dioxane per mole PRCHC and is unstable under ambient conditions. Desolvation (thermally or at relative humidities >40%) of the dioxane solvate results in the metastable polymorphic form mod. II.

The amorphous form arises from freeze-drying of an aqueous solution (5% PRCHC) and contains about 4% water at ambient conditions.

*Characterization of the different solid phases*

Thermal analysis

Hot-stage microscopy

The commercial product consists of 100 to 500 μm long (Fig. 2a), highly birefringent stems of the stable form mod. I°. Upon heating, the crystals of mod. I° sublime above 140°C to capillary needles and stems. Mod. I° melts at 169°C, which coincides with the literature data. The melt does not recrystallize on cooling unless the crystallization is induced by seeding with the original crystals at any temperature between 135°C and the melting point. Mod. I° grows from the melt as spherulites composed of fine needles. Neither the nucleation of mod. II nor any solid–solid transformation can be observed by hot-stage microscopy.

The dioxane solvate forms transparent, tabular crystals (Fig. 2b) loosing their transparency within three days of storing (Fig. 2c). On heating, the crystals start to melt at about 108°C and the formation of bubbles in the liquid can be observed. Due to fast recrystallization processes to the anhydrous solid at the surface, the original shape of the crystals is more or less maintained after this inhomogeneous melting process. The process ends at about 125°C and results in opaque particles (Fig. 3). On further heating the desolvated particles start to melt at 165°C. The majority of the solid melts below 168°C (mod. II) whereas another crystalline part (mod. I°) melts between 169 and 170°C.

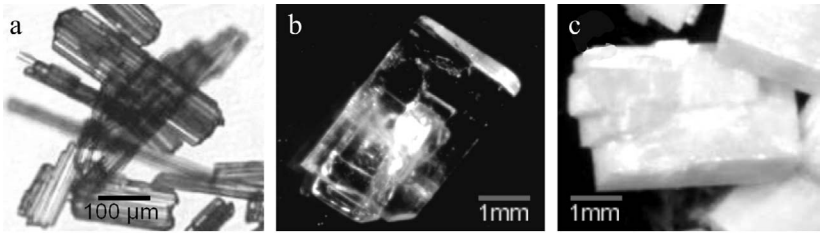


**Fig. 2** Micrographs of PRCHC crystal phases: a – commercial prodcut (mod. I°), b – dioxane solvate crystal freshly crystallized and c – after 3 days at room conditions (mod. II)

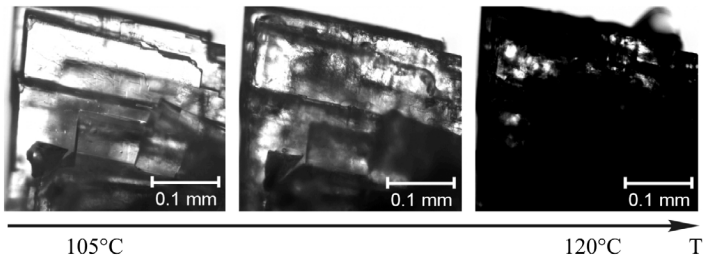


**Fig. 3** Micrographs of a PRCHC dioxane solvate crystal desolvating at 105–120°C

The amorphous form shows transparent, non birefringent chunks. On heating up to 70 to 90°C the crystallization of capillary needles of mod. I° can be observed, which melt at 169°C.

## Differential scanning calorimetry

Figure 4 shows the DSC curves of the three crystal forms and in Table 1 the thermophysical data are summarized. Mod. I° exhibits only a narrow endothermic melting peak with an onset of 169.0°C. The dioxane solvate shows an inhomogeneous melting process between 108 and 125°C, i.e. it partly melts, desolvates and crystallizes simultaneously which is indicated by a broad endothermic peak followed by an exothermic process. On further heating a mixture of mod. II and mod. I° can be identified by their melting peaks. Freshly prepared single crystals of the solvate transform to mainly mod. II upon heating in an aluminium pan with perforated cover, whereas milled crystals yield more of

mod. I°. However, when the dioxane solvate is desolvated at 140°C in an oven, the DSC-curve shows the melting peak of mod. II only (Fig. 4, curve 1).

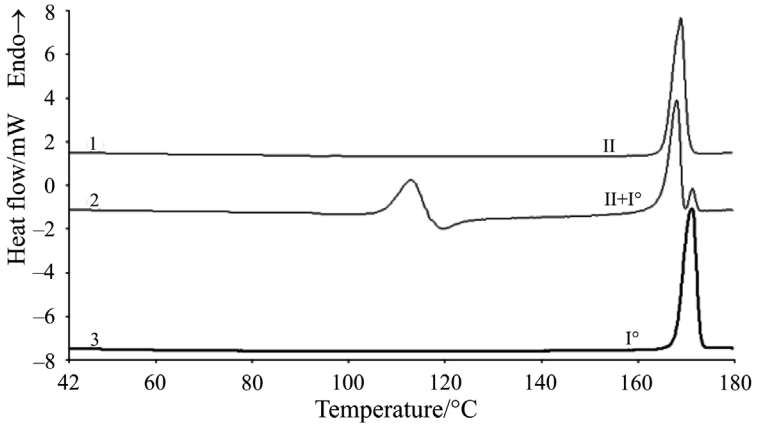


**Fig. 4** DSC curves of PRCHC crystal forms prepared in sample pans with perforated covers. 1 – PRCHC mod. II, dioxane solvate kept at 140°C for 12 h; 2 – PRCHC dioxane solvate heated in a pan with pereforated cover: desolvation and crystallization process at 105–120°C followed by the melting endotherms of a mod. II/I°mixture (ratio 8:1, calculated on the fusion enthalpies); 3 – PRCHC mod. I°, commerical batch. Heating rates: 5 K $min^{-1}$

The DSC curve of the amorphous form (not shown) shows an exothermic peak at about 70°C (crystallization of mod. I°) followed by a melting endotherm at 169°C (melting of mod. I°).

## Thermogravimetric analysis

The TG curves of the commercial crystals and the desolvated dioxane solvate (mod. II) show only a weak but continuous mass loss above 120°C caused by sublimation. The TG curves of the dioxane solvate (Fig. 5) exhibit a distinct step at about 115°C due to the loss of the solvent. Powdered crystals of the solvate start to slowly desolvate already at about 75°C whereas the onset of desolvation of single crystals of the solvate can be observed at about 110°C. The relative mass loss of 14.7% corresponds to exactly 0.50 mole 1,4-dioxane per mole PRCHC, clearly proving the presence of a stoichiometric hemisolvate.

The amorphous form, stored three days at ambient conditions, contains about 4% water, which in the dry nitrogen purge in TG starts to escape already at 30°C.

## Spectroscopy

### FTIR- and Raman-spectroscopy

Both, FTIR- (Fig. 6) and Raman-spectra (Fig. 7) of the individual solid forms show clear differences. The most striking differences can be realized in the range of the

**Table 1** Physicochemical data of PRCHC solid-state forms

| Solid-state form | Mod. I° | Mod. II | Dioxane solvate | Amorphous form |
|---|---|---|---|---|
| Production | commercial product, crystallization from most organic solvents | desolvation of the dioxane solvate at 140°C | crystallization from 1,4-dioxane | lyophilization of an aqueous solution (5%) |
| Melting point/°C | 169±1.0 | 165.5±0.5 | 108 | |
| Enthalpy of fusion/kJ $mol^{-1}$ ±95% c.i. | 31.9±0.1 | 29.5±0.2 | desolvation and recrystallization | |
| IR data/$cm^{-1}$, νN–H | 3204 | 3210 | 3186 | |
| Order of thermodyn. stability of polymorphs at 20°C | 1 | 2 | | |
| Max. water vapor sorption at 90% RH/%* | 0.04±0.01 | 0.14±0.02 | 0.16 (mod. II) | 1.73 (after partial crystallization to mod. I°) |
| Kinetic stability (storage, 20 to 25°C, 40 to 55% RH) | always stable | >1 year | few days (transformation to mod. II) | few weeks (cryst. to mod. I°) |

c.i.. confidence interval; *mass change in % relating to the sample mass at 0% RH

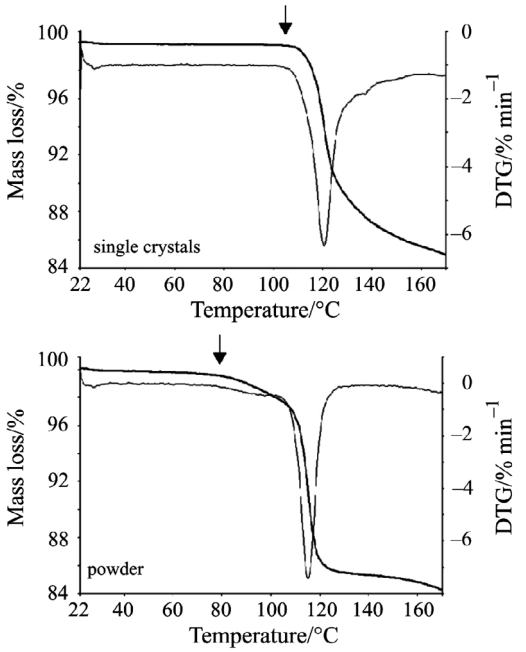


**Fig. 5** TG and derivative TG curves of prilocaine hydrochloride dioxane solvate samples. The desolvation process of a powdered sample (lower plot) starts earlier than in single crystals (marked by arrow) and is finished before sublimation starts at 140°C. Heating rate 5 K min$^{-1}$

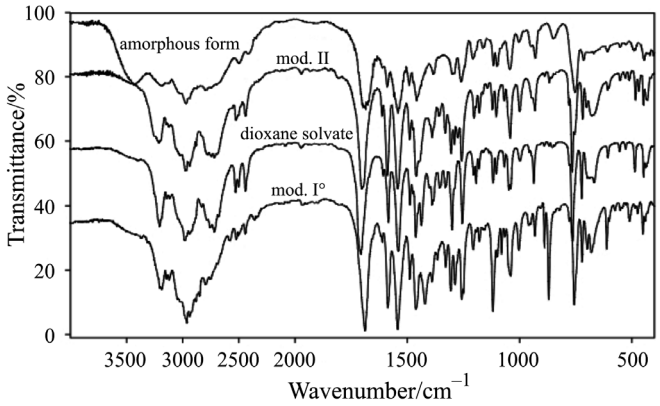


**Fig. 6** FTIR spectra of PRCHC solid-state forms (KBr method)

C–H stretching vibrations of the alkyl chain (2980 to 2960 cm$^{-1}$, Raman), the valence vibrations of the carbonyl and amine group (1700 to 1600 cm$^{-1}$, FTIR), the molecule vibrations (1500 to 1000 cm$^{-1}$, FTIR) and the lattice vibrations (200 to 50 cm$^{-1}$,

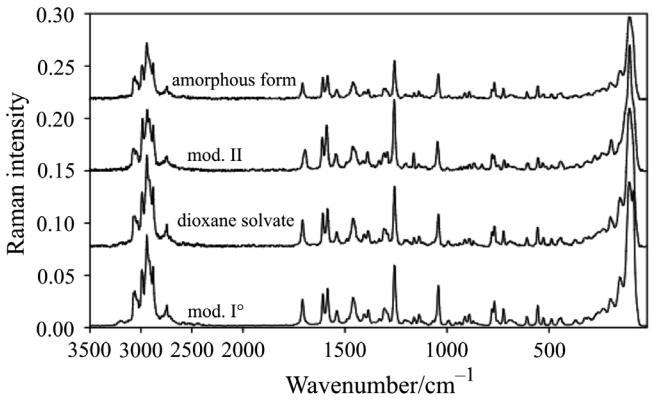


**Fig. 7** FT-Raman spectra of PRCHC solid-state forms

Raman). The characteristic IR absorption bands of the different forms are shown in Table 2. The amorphous form shows weaker and broad peaks and an additional peak at 3422 cm$^{-1}$ due to the presence of water. A sample of the amorphous form prepared on a ZnSe-disk and heated to 100°C showed the spectrum of mod I°.

The N–H stretching vibration (FTIR) of the stable form (mod. I°) is at lower wavenumbers (3204 cm$^{-1}$) than that of the metastable mod. II (3210 cm$^{-1}$). This is in accordance with the IR-rule [18, 19] and suggests that intermolecular hydrogen-bonding to the N1 amino-function plays an important role in the molecular ar-

**Table 2** Characteristic infrared frequencies and assignments for PRCHC solid-state forms

| Mod. I°/cm$^{-1}$ | Mod. II/cm$^{-1}$ | Dioxane solvate/cm$^{-1}$ | Amorphous form/cm$^{-1}$ | Assignment |
|---|---|---|---|---|
| | | | 3422 (m) | νO–H* |
| 3204 (s) | 3210 (m) | 3186 (m) | 3190 (m) | νN–H |
| 2976 (s) | 2967 (s) | 2962 (s) | 2969 (m) | νC–H |
| 2753 (s) | 2744 (s) | 2794 (m) | 2794 (m) | νN–H |
| 1705 (s) | 1703 (s) | 1690 (s) | 1696 (m) | νC=O |
| 1607 (m) | 1612 (m) | 1611 (m) | 1606 (m) | νC–N |
| 1584 (s) | 1589 (s) | 1586 (s) | 1589 (m) | νC–C |
| 1540 (s) | 1542 (s) | 1542 (s) | 1540 (m) | δC–H |
| 1300 (s) | 1305 (s) | 1306 (m) | 1291 (m) | fingerprint |
| 1103 (m) | 1104 (m) | 1100 (m) | 1099 (m) | |
| 998 (w) | 999 (m) | 959 (w) | 1002 (w) | δN–H |
| 852 (w) | 868 (w) | 870 (s) | 849 (w) | |
| 761 (s) | 766 (s) | 757 (s) | 752 (m) | |
| 606 (w) | 608 (w) | 611 (m) | 607 (w) | |

*water; s. strong (>70%T), m. medium (40–70%T), w. weak (<40%T)

rangements of the two crystal forms. The lattice vibrations in the region below 200 $cm^{-1}$ (Raman) clearly reflect the different crystal structures of the three forms.

Powder X-ray diffractometry (PXRD)

The X-ray powder patterns of the crystal forms are illustrated in Fig. 8 and the most important positions and relative intensities are listed in Table 3. The diffractograms of mod. I° and II are very different and allow a clear and fast identification of the polymorphs.

The amorphous form shows a typical halo, but after storage at ambient conditions for 14 days, some small peaks of mod. I° can be observed. Temperature-controlled PXRD of the amorphous form at 100°C resulted in pure mod. I° (Fig. 9). From moisture-controlled PXRD studies it is obvious, that raising of the relative humidity above 40% RH also induces a fast crystallization to the stable mod. I°.

*Thermodynamic and kinetic stability of PRCHC solid-state forms*

Table 1 summarizes the most important thermodynamic data of the solid-state forms as well as the wavenumbers of the νN–H IR-modes. The thermodynamic relationship of the PRCHC solid-state forms is displayed in the semi-schematic energy/temperature-diagram [20] in Fig. 10 along with a scheme showing the possible transition pathways between the forms. Since mod. I° has a higher enthalpy of fusion than mod. II, the two polymorphs are monotropically related (heat of fusion rule [18, 21]) and thus the higher melting mod. I° is the thermodynamically stable form in the entire temperature range. However, samples of mod. II, stored in glass vials at ambient conditions for a

**Table 3** Most important two theta positions (2θ/°), *d*-spacings (*d*) and relative intensities (*I*) of the powder X-ray diffraction patterns of PRCHC crystal forms

| Mod. I° | | | Mod. II | | | Dioxane solvate | | |
|---|---|---|---|---|---|---|---|---|
| °2θ | *d*/Å | *I*/% | °2θ | *d*/Å | *I*/% | °2θ | *d*/Å | *I*/% |
| 6.744 | 13.0961 | 80.98 | 3.580 | 24.6604 | 67.08 | 6.585 | 13.4122 | 100.00 |
| 7.019 | 12.5829 | 100.00 | 7.286 | 12.1223 | 100.00 | 11.478 | 7.7032 | 77.00 |
| 7.350 | 12.0174 | 9.59 | 12.122 | 7.2952 | 84.05 | 12.097 | 7.3100 | 30.32 |
| 14.098 | 6.2770 | 7.46 | 16.238 | 5.4542 | 48.53 | 13.208 | 6.6978 | 21.88 |
| 14.830 | 5.9684 | 48.96 | 18.430 | 4.8101 | 56.17 | 19.148 | 4.6313 | 29.70 |
| 22.916 | 3.8776 | 8.89 | 18.684 | 4.7453 | 75.32 | 19.925 | 4.4524 | 37.94 |
| 24.657 | 3.6076 | 19.38 | 20.457 | 4.3377 | 51.26 | 20.987 | 4.2293 | 28.66 |
| 25.700 | 3.4635 | 9.80 | 22.805 | 3.8961 | 48.33 | 22.767 | 3.9026 | 36.07 |
| 27.220 | 3.2735 | 53.50 | 24.886 | 3.5749 | 69.39 | 24.365 | 3.6502 | 27.98 |
| 34.798 | 3.5760 | 8.73 | 25.694 | 3.4643 | 60.26 | 24.720 | 3.5986 | 28.52 |
| 35.233 | 2.5452 | 7.58 | 27.590 | 3.2304 | 67.62 | 26.893 | 3.3125 | 28.28 |

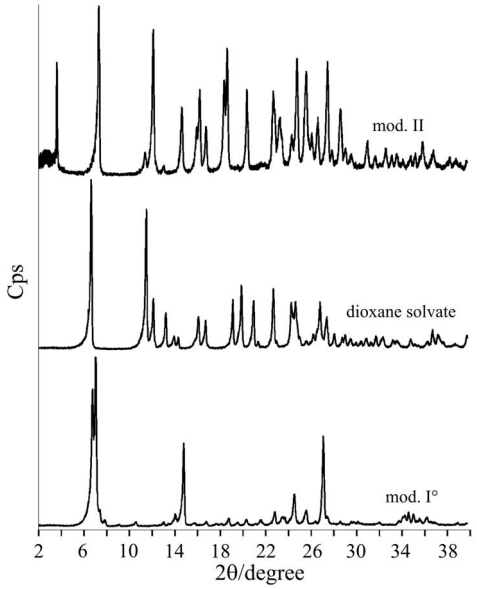


**Fig. 8** Powder X-ray diffraction patterns of PRCHC crystal forms at 20°C

year did not transform to the stable mod. I° (confirmed by DSC and PXRD). This testifies, that the kinetic stability of mod. II is high.

The amorphous form starts to crystallize to the stable mod. I° within a few weeks, whereas the dioxane solvate crystals desolvate already within a few days to the metastable mod. II.

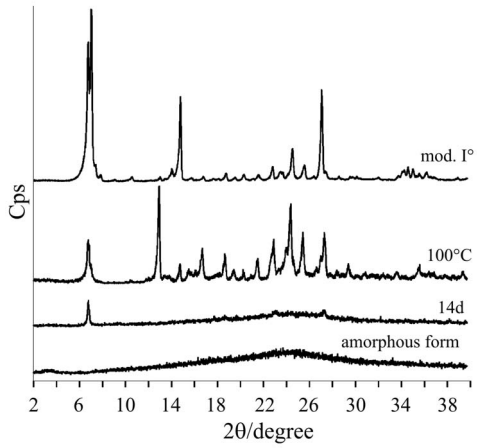


**Fig. 9** Powder X-ray diffraction patterns of PRCHC showing the crystallization of the amorphous form (bottom) to mod. I° (pure form at the top) after 14 days of storage at room conditions (14d) and at 100°C (100°C). The differences in the peak intensities of the upper patterns are attributed to preferred orientation

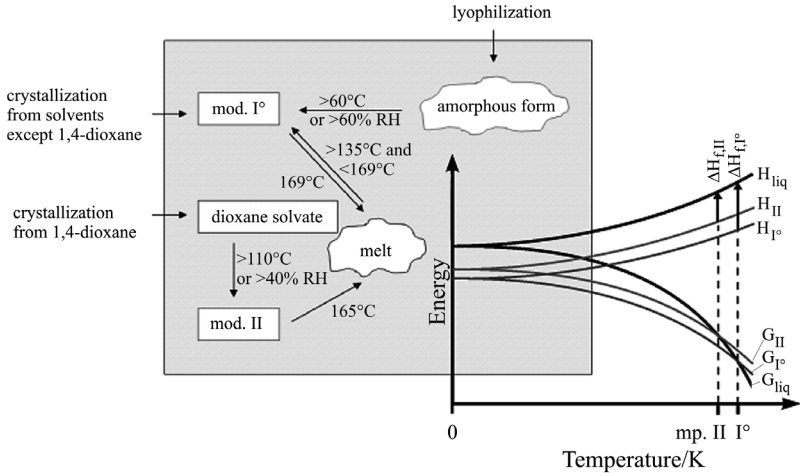


**Fig. 10** Flow chart of PRCHC solid-state forms and melt with transformation temperatures under ambient pressure conditions (left) and semischematic energy/temperature-diagram of the polymorphs (right). *H* – enthalpy, *G* – Gibbs free energy, $\Delta H_f$ – heat of fusion, liq: liquid phase (melt)

## *Moisture sorption*

The solid-state forms differ also in their moisture sorption behaviour. Figure 11 shows the moisture sorption isotherms of the four different solid forms, which can be a very useful tool to differentiate and identify the forms or rank polymorphic forms

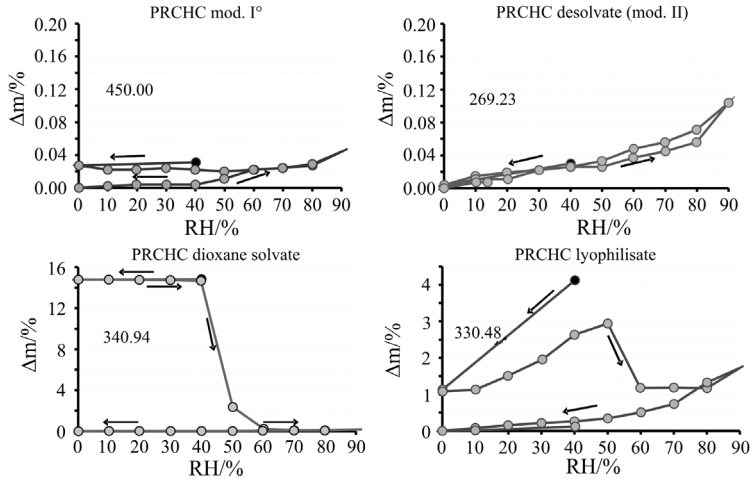


**Fig. 11** Moisture sorption isotherms of PRCHC solid-state forms at 25°C. The mass change is corrected for the minimum mass value of 0% RH. The measurement cycle started at 40% (dark point). The numbers within the diagrams show the net masses of the sample at the start of the cycle

by their relative thermodynamic stability (with regard to surface area and crystal transformations). Mod. I°, the thermodynamic and kinetic most stable form, adsorbs the smallest amount of water at 90% RH (Table 1), whereas the metastable mod. II shows a threefold higher value. The dioxane solvate shows a mass loss of nearly 15% at 50% RH followed by an isotherm which is similar to that of the pure mod. II. As expected, the amorphous form is the most hygroscopic solid form. The moisture sorption isotherm shows a mass loss at 60% RH which confirms the partial crystallization of the amorphous form to mod. I° (proved also by moisture controlled PXRD).

## Conclusions

PRCHC forms two monotropically related polymorphs (mod. I° and mod. II), a dioxane-solvate with 0.5 mole solvent per mole PRCHC and an amorphous form. The metastable mod. II can only be obtained by desolvation of the dioxane-solvate and exhibits a high kinetic stability (at least one year) at ambient conditions. So this polymorph may also be suitable for the production of solid drug formulations. Freeze-drying of a PRCHC solution results in an amorphous form, which is physically unstable and crystallizes to the stable mod. I° at elevated temperatures or relative humidities.

Since PRCHC is a drug compound with high solubility in water, the existence of a metastable form with high kinetic stability (mod. II) is probably of low practical relevance. However, PRCHC represents an example for a polymorphic system where a certain polymorphic form does not directly nucleate from the supercooled melt, the glass or solvents, but can only be obtained via a specific solvate. In earlier solid-state studies on PRCHC (describing this compound as monomorphic) obviously no crystallization in 1,4-dioxane was performed and therefore the solvate and finally the new polymorph (mod. II) could not be found. In order to find as many polymorphs as possible it is thus very important to crystallize a compound from a large number of solvents and to properly characterize existing solvates and their desolvation products.

* * *

The authors would like to thank Ing. E. Gstrein for technical assistance.

## References

1 H. Goodman and F. Gilman, Pharmakologische Grundlagen der Arzneimitteltherapie, McGraw-Hill, Frankfurt 1998, p. 345.
2 A. C. Schmidt, N. Senfter and U. J. Griesser, J. Therm. Anal. Cal., 73 (2003) 401.
3 A. C. Schmidt, U. J. Griesser, T. Brehmer, R. K. Harris and A. King, Acta Cryst., A58 (2002) C140.
4 A. C. Schmidt, U. J. Griesser and K. Mereiter, Workshop-Konferenz Kristallzucht, Messtrategien, Kristallkonstruktion und Polymorphie, Essen 2001.
5 A. C. Schmidt and U. J. Griesser, Sci. Pharm., 71 (2003) 89.
6 A. C. Schmidt and U. J. Griesser, PhandTA 7 (7th Int. Conf. /Workshop on Pharmacy and Applied Phys. Chem.), Eurostar Meeting, Innsbruck 2003.

7 V. Niederwanger, A. C. Schmidt and U. J. Griesser, PhandTA 7 (7th Int. Conf. /Workshop on Pharmacy and Applied Phys. Chem.), Eurostar Meeting, Innsbruck 2003.
8 U. Rohregger, Diploma Thesis, Innsbruck 1999.
9 http://www.astrazeneca.com/productbrowse/4_69.aspx.
10 M. Kuhnert-Brandstätter, A. Kofler and G. Kramer, Sci. Pharm., 42 (1974) 156.
11 D. Giron, M. Draghi, C. Goldbronn, S. Pfeffer and P. Piechon, J. Thermal Anal., 49 (1997) 913.
12 A. W. Hanson and D. W. Banner, Acta Cryst., B30 (1974) 2486.
13 A. W. Hanson and M. Rohrl, Acta Cryst., B28 (1972) 3567.
14 B. S. Hayward and J. Donohue, J. Cryst. Mol. Struct., 7 (1977) 275.
15 I. Csöregh, Acta Cryst., C48 (1992) 1794.
16 H. J. Bruins, H. J. Behm and H. E. M. Kerkkamp, Acta Cryst., B46 (1990) 842.
17 H. A. Rose, Acta Cryst., 8 (1955) 65.
18 A. Burger and R. Ramberger, Microchim. Acta, 2 (1979) 308.
19 A. Burger and R. Ramberger, Microchim. Acta, 2 (1979) 265.
20 A. Grunenberg, J. O. Henck and H. W. Siesler, Int. J. Pharm., 129 (1996) 147.
21 L. Yu, J. Pharm. Sci., 84 (1995) 969.